

8<sup>th</sup> COST260 MCM, Rennes, France, 1-3<sup>rd</sup> October 2000

## SPATIAL DE-CORRELATION OF THE UTRA-FDD RADIO CHANNEL

Ben Allen<sup>(1)</sup>, Mark Beach<sup>(1)</sup> and Peter Karlsson<sup>(1)</sup><sup>(1)</sup>Centre for Communications Research,

University of Bristol, Queen's Building, Woodland Road, Bristol BS8 1TR

Tel: +44 (0) 117 9288617, Fax: +44 (0) 117 9545206,

E-Mail: [Ben.Allen@bristol.ac.uk](mailto:Ben.Allen@bristol.ac.uk)

### Abstract

For smart antenna deployment in Frequency Division Duplex (FDD) applications the downlink weight vector can be derived from the uplink steering vector, assuming a degree of correlation between these channels. It is shown here that de-correlation between uplink and downlink power azimuth spectrums (PAS) is significant for frequency offsets as small as 5MHz in urban environments. Results reported here are computed from measured data taken within the UTRA (UMTS Terrestrial Radio Interface) frequency band for cluttered urban.

### I INTRODUCTION

Smart antennas are now regarded by many as a core system component within future wireless networks in order to meet the demands for high capacity [1]. For applications such as W-CDMA (Wideband Code Division Multiple Access) in UTRA (UMTS Terrestrial Radio Air-interface) which employs a Frequency Division Duplex (FDD) air interface, the smart antenna may derive downlink weights from the uplink PAS (Power Azimuth Spectrum) characteristics of the channel. Such blind downlink beamforming schemes are reported in [2-7]. For robust operation of these schemes it is important to consider the spatial correlation between uplink and downlink for the numerous operational environments associated with W-CDMA.

This paper first describes an urban propagation measurement campaign that has been conducted within the UMTS band. A novel technique for computing the spatial correlation bandwidth is then presented and results are computed using the urban trials data for an angular resolution of 2°. Finally, the impact of reduced angular resolution is investigated.

### II MEASUREMENT SYSTEM

The measurement system employed a state-of-the-art wideband vector channel sounder (Medav RUSK BRI [8]) configured to operate over a 20MHz bandwidth centred on 1920MHz. The mobile station (MS) transmitter continuously emitted a periodic multi-tone signal and employed a commercially available 2dBi gain omni-directional sleeve dipole slanted at 45° on top of the test vehicle and auxiliary +40dBm power amplifier. The receiving antenna was a dual polarised facet from Allgon Antennas (figure 1) consisting of 8 sub-array panels spaced apart by  $0.544\lambda$ , each providing a 3dB azimuth beamwidth of 120° and some 17dBi of elevation gain. The array had no electronic down-tilt, hence mechanical down-tilt was employed during the trials. A customised high-speed multiplexer provided the interface between the 16 output ports on the Allgon array and the Medav RUSK receiver input as well as additional amplification and channel filtering (shown in figure 1b). Multiplexing took place in 2 stages; a 16:8 multiplexer provided polarisation switching which was followed by an 8:1 multiplexer to switch between the sub-arrays. The receiver data logging system therefore recorded 8 channel impulse responses (CIRs) for the +45° polarisation and 8 for the -45° polarisation where 8 CIRs taken across the array is a *snapshot*. This was repeated so that 2 snapshots were recorded for each polarisation (required for accurate direction of arrival estimation), giving a total of 32 snapshots, known as a Fast Doppler Block (FDB). The associated received signal structure is shown in figure 2 where the total received signal period is assumed to be less than 6.4µs was used for the urban trials. The results presented here have only considered data received on the +45° polarisation therefore leaving 16 snapshots per FDB. Polarisation de-interleaving took place during post-processing. A unique feature of this system was that a complete dual polar received complex channel response was taken across the array within the coherence time of the channel (here the measurement period was 204.8µs which is shorter than the time period of one slot in UTRA-FDD of 667µs).

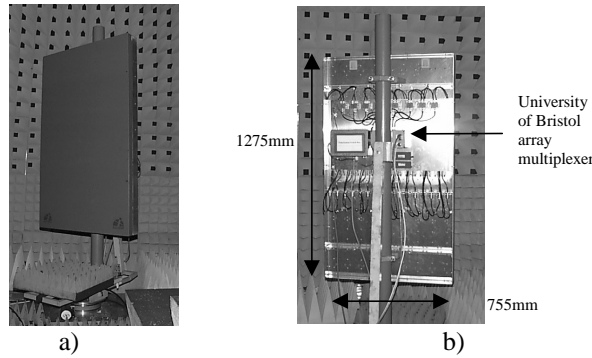


Fig 1. The Allgon , dual polarised receiving array during calibration.  
a) Front b) Back

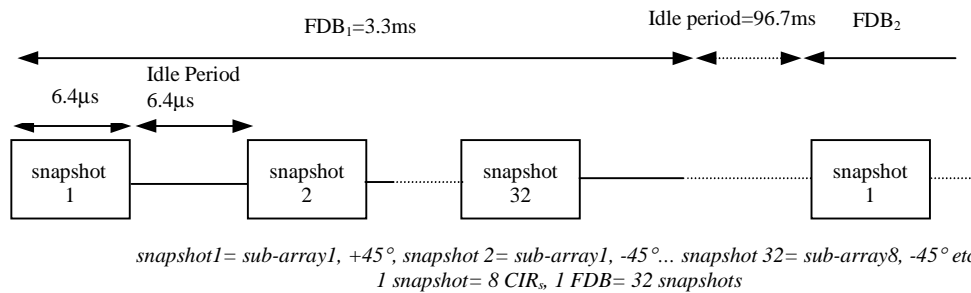
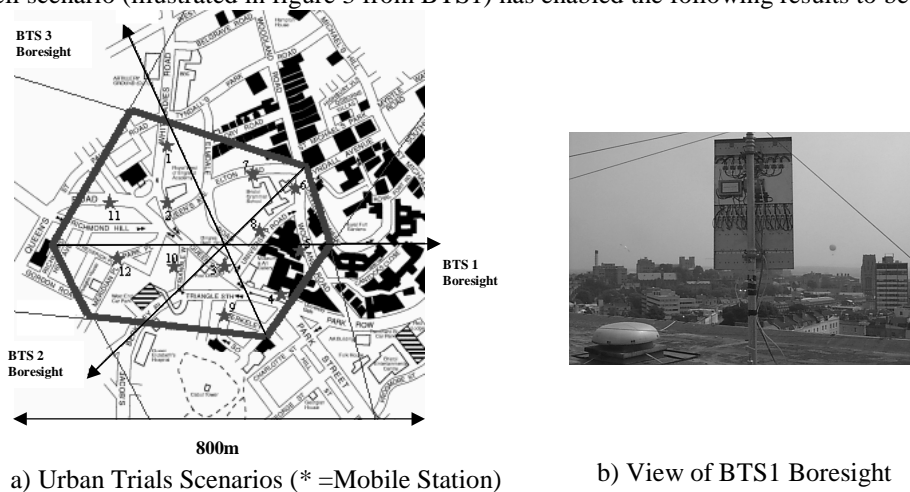


Fig 2. Received Signal Structure

Prior to deployment the system was calibrated to ensure that only channel characteristics were measured. Temporal calibration required the transmitter and receiver frequency references and system clocks to be coherently aligned allowing accurate phase and time-of-flight estimates to be made. Spatial calibration was by means of estimating the receiving array mutual coupling matrix in an anechoic chamber. The procedure consisted of measuring the 8 sub-array azimuth patterns and then estimating the correction matrix by means of the least squares algorithm described in [9]. This has allowed direction of arrival estimation accuracy of better than 1° to be recorded [10] and has enabled full verification of the results presented in the following sections.

### III TRIALS CAMPAIGN

The system was used to measure complex channel responses for all combinations of 3 rooftop basestation (BTS) locations and 12 mobile locations in the Clifton area of Bristol. Mechanical down-tilts of 5°, 7.5° and 5° was applied at the BTS locations respectively to ensure coverage of the area shown in figure 3. At each location 100 FDB<sub>s</sub> were recorded over a 10s period. The MS locations were uniformly distributed over the cell with ranges of between 50m and 650m between the MS and BTS as shown in figure 3. Post processing of the measured data for this small, heavily cluttered urban cell scenario (illustrated in figure 3 from BTS1) has enabled the following results to be obtained.



a) Urban Trials Scenarios (\* =Mobile Station) b) View of BTS1 Boresight  
Fig 3. Trials Scenarios

#### IV ANALYSIS

The PAS was computed over a 5MHz bandwidth using 16 snapshots (1 FDB) recorded whilst the MS was stationary (in contrast to a moving MS used in the measurement campaign reported in [11]) where averaging took place over the entire impulse response to remove wideband fading artifacts. The 1D unitary ESPRIT algorithm [12] was employed with a 15dB dynamic range, 120° azimuth window and an angular resolution of approximately 2° to compute the resultant PAS. Computation was repeated for each frequency offset (0 to 15MHz in 156.25kHz steps). The correlation coefficient ( $\rho_{ij}$ ) was then computed between each PAS pair using equation 1.

$$\rho_{ij} = \frac{R_{ij}}{\sqrt{\left[ \sum_{n=0}^{N-1} x_i^2(\theta_n) \cdot \sum_{n=0}^{N-1} x_j^2(\theta_n) \right]}} \quad (1)$$

Where  $R_{ij}$  is the cross correlation at zero lag of the PAS  $x_i(\theta)$  and  $x_j(\theta)$  sampled at angles  $\theta_n$ . An  $I \times J$  correlation coefficient matrix containing the correlation coefficients for each PAS pair can then be constructed, an example of which is shown in figure 5a for the channel data obtained between BTS1 and MS8 in figure 3a. The matrix clearly shows the auto-correlation along the diagonal. Symmetry occurs about this diagonal since  $\rho_{ij}=\rho_{ji}$ , thus the required correlation data is contained within the lower-right half of the matrix.

By averaging over each diagonal, the PAS correlation can be determined as a function of frequency offset as shown in figure 5b. By selecting a correlation coefficient threshold ( $\rho_{th}$ ), the PAS correlation bandwidth ( $B_\theta$ ) can be determined. The result in figure 5 yields  $B_\theta=5.5\text{MHz}$  for  $\rho_{th}=0.5$  and  $B_\theta=412\text{kHz}$  for  $\rho_{th}=0.9$  respectively for the operational environment given in figure 3.

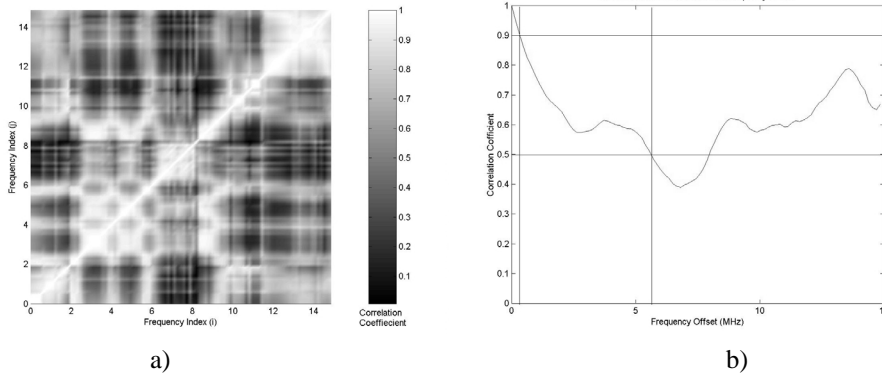


Fig 5. a) Example Spatial Correlation Coefficient Matrix (urban site)  
b) Average PAS Correlation versus Frequency Offset

The PAS de-correlation is apparent in figure 6a, where the differences between uplink and downlink PAS are shown for the channel between MS1 and BTS1. The PAS is shown graphically in figure 6b as a function of incremental frequency offset. A significant change in PAS is seen for frequency offsets of more than 4MHz. The changes shown in figure 6 illustrate the requirement for robust downlink beamforming. The application of a blind downlink optimum combiner solution in such an environment is likely to fail for duplex spacing of greater than  $B_\theta$  as the perceived directions of departure will be sub-optimum.

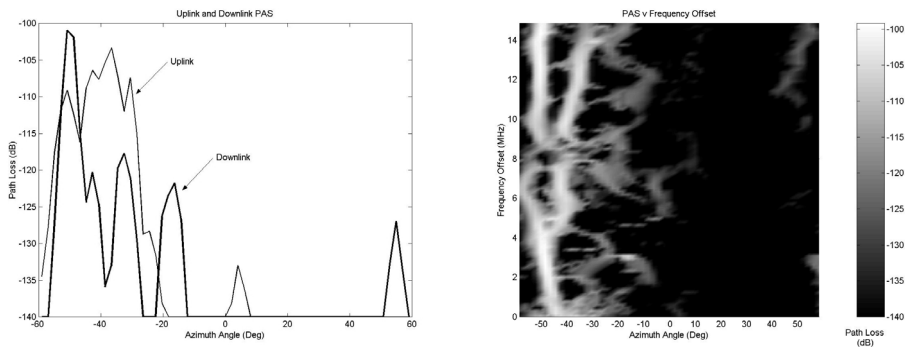


Fig 6. a) Uplink and Downlink PAS  
b) PAS as a Function of Incremental Frequency Offset

By repeating the above procedure for each of the 100 FDBs and for each BTS and MS location, the probability density function (PDF) of PAS correlation bandwidth is computed. The resulting PDF's are given in figure 7a. For  $\rho_{th}=0.5$ , the median spatial correlation bandwidth is computed to be 5MHz. For a small number of cases PAS correlation bandwidths of greater than 10MHz have been reached. For  $\rho_{th}=0.9$ , the median spatial correlation bandwidth is reduced to 412kHz.

An angular resolution of  $2^\circ$  has been used so far. This is considered too fine as applications utilising an 8 element array yield a much lower beamforming resolution. The computations have therefore been repeated using a more realistic angular resolution of  $16^\circ$  which yields median  $B_\theta=12.5\text{MHz}$  and  $2\text{MHz}$  for  $\rho_{th}=0.5$  and  $0.9$  respectively. The resulting PDF's are shown in figure 7b.

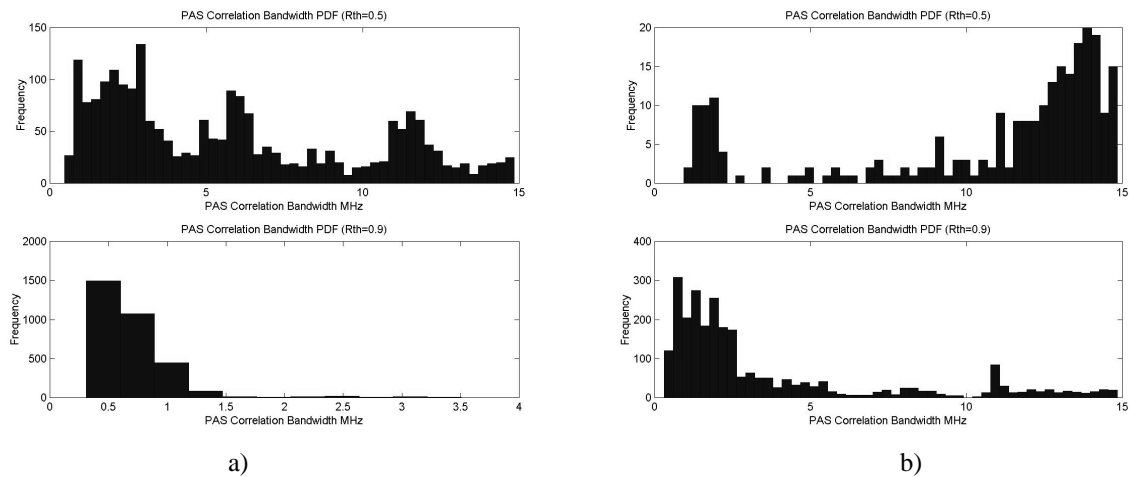


Fig 7: PDF of PAS Correlation Bandwidth  
a) Angular Resolution of  $4^\circ$       b) Angular Resolution of  $32^\circ$

## V CONCLUSIONS

The spatial channel parameters obtained from a trials campaign centered at 1920MHz has enabled the spatial correlation bandwidths of the measurements environments to be computed. Results using an angular resolution of  $2^\circ$  yields median  $B_\theta=5\text{MHz}$  for  $R_{th}=0.5$ . It is shown that by using a more realistic angular resolution of  $16^\circ$ , median  $B_\theta$  is increased to 12MHz.

## VI ACKNOWLEDGEMENTS

The authors are grateful to colleagues at the CCR and in particular Julian Webber for leading the indoor and outdoor-indoor measurement campaigns. The authors gratefully acknowledge funding support under HEFCE JREI'98 and Allgon Systems AB for the loan of the antenna array.

## REFERENCES

- [1] Y J.Guo, S Vadgama, Y Tanaka, "Advanced Base Station Technologies for UTRAN", IEE Electronics and Communications Engineering Journal, Vol. 12, No. 3, June 2000, pp123-132
- [2] J Goldberg, J Fonollosa, "Downlink Beamforming for Spatially Distributed Sources in Cellular Mobile Communications", Signal Processing, Special Issue on Distribution Theory in Signal Processing, EURASIP, Vol. 65, No. 2, pp181-197, March 1998
- [3] G Raleigh, S Diggavi, V Jones, A Paulraj, "A Blind Adaptive Transmit Antenna Algorithm for Wireless Communications", Proceedings of IEEE International Communications Conference, 1995, pp1494-1499
- [4] C Farsafh, A Nossek, "Spatial Covariance Based Downlink Beamforming in an SDMA Mobile Radio System", IEEE Transactions on Communications, Vol. 46, No. 11, 1998, pp1497-1506
- [5] B Lindmark, M Ahlberg, M Nillson, C Beckman, "Performance Analysis of Applying Uplink Estimation in the Downlink Beamforming Using a Dual Polarised Array", Proceedings of IEEE VTC, Spring 2000, Tokyo, Japan

- [6] K Hugl, J Laurila, E Bonek, "Downlink Performance of Adaptive Antennas with Null Broadening", Proceedings of IEEE VTC, Spring 1999, Houston, Texas
- [7] J Thampson, J Hudson, P Grant, B Mulgrew, "CDMA Downlink Beamforming for Frequency Selective Channels", Proceedings of IEEE PIMRC 1999, Japan
- [8] R Thomä, D Hampicke, A Richter, G Sommerkorn, A Schneider, U Trautwein and W Wirthner, "Identification of Time-Variant Directional Mobile Radio Channels" IEEE Trans. Instrumentation and Measurement, Vol. 49, No. 2, April 2000, pp357-364
- [9] G Sommerkamp, D Hampicke, R Klukas, A Richter, A Schneider, R Thomä, "Reduction of DOA Estimation Errors Caused by Antenna Array Imperfections", Proceedings of the 29<sup>th</sup> European Microwave Conference, Munich, October 5-7, 1999, pp282-290
- [10] M Beach, D McNamara, P Karlsson, "Development of a Channel Measurement System for Multiple-Input Multiple-Output (MIMO) Applications", Submitted to IST Mobile Summit, Galway, Eire, October 2000
- [11] K Pedersen, P Mogensen, F Frederiksen, "Joint Directional Properties of Uplink and Downlink Channel in Mobile Communications", IEE Electronics Letters, Vol. 35, No.16, August 1999, pp1311-1312
- [12] Martin Haardt, Josef A.Nossek, "Unitary ESPRIT: How to obtain Increased Estimation Accuracy With Reduced Computational Burden", IEEE Transactions on Signal Processing, Vol. 43, No. 5, May 1995, pp1232-1242